Available online www.jsaer.com

***Journal of Scientific and Engineering Research*, 2021, 8(12):158-171**

Research Article

ISSN: 2394-2630
CODEN(USA): JSERBR

Study of the Stability of the Inter-Connected Electrical Network Following the Injection of Energy from Solar Photovoltaic Power Plants: Case of the Electrical Network of Burkina Faso

Arnaud OUERMI[1], Alassane DIENE, Sié KAM[2], Mamadou WADE[1], Dieudonné Joseph BATHIEBO[2]

[1]Laboratory of Water and Environmental Science and Technology, ' LaSTEE; Thiès Polytechnic School (EPT), BP 10A, Thiès, Senegal
[2]Laboratory of Thermal and Renewable Energies, 'LETRE'; Joseph KI-ZERBO University, UJKZ, 03 B.P. 7021, Ouagadougou, Burkina Faso

Abstract Faced with the energy deficit in sub-Saharan African countries and the depletion of fossil energy sources, Burkina Faso is planning to build several solar photovoltaic power plants that will be integrated into the National Interconnected Electricity Network (NIEN). This work is part of the analysis of the impact in terms of degradation or disruption of these facilities on the electrical network

First, the NIEN of BURKINA FASO was modeled on the "Digsilent Power Factory" software with all its power plants in operation.

Then, simulations of the Network Constraining Scenarios (NCS) were performed in order to identify the levels of voltage degradation and the additional short circuit current contribution following the injection of energy from the operating and planned solar photovoltaic power plants.

The analysis of the simulation results shows that following the injection of energy from the solar power plants, the power flows and short-circuit currents are greatly modified (increase, decrease and reversal of direction) at the majority of the busbars. These modifications require the electrical network to readapt its protection equipment, as well as to modernize the SONABEL dispatching center and communication system.

Finally, reinforcement of the equipment at the different points of the network with overloads has been proposed in order to obtain a network in good working condition.

Keywords Stability, National Interconnected Network (NIN); solar; injection, power flow, short circuit current

Nomenclature

Symbol	Designation	Unit
P_c	Peak power	Watt-peak (Wp)
P_p	Peak power	Megawatt (MW)
T_P	Penetration rate	Percentage (%)
P	Instantaneous power	Megawatt (MW)
G	Global irradiation received in the plane of the solar PV modules	Kilowatt-hour per square metre per day (kWh/m^2.d)
η	overall PV system efficiency	
S_i	Apparent power at node i	Megavolt-Ampere (MVA)
P_i	Active power at node i	Megawatt (MW)
Q_i	Reactive power at node i	MVAR

S_{Gi}	Apparent power generated at node i	Megavolt-Ampere (MVA)
S_{Di}	Apparent power demand at node i	Megavolt-Ampere (MVA)
P_{Gi}	Active power generated at node i	Megawatt (MW)
P_{Di}	Active power demand at node i	Megawatt (MW)
Q_{Gi}	Reactive power generated at node i	Megavolt-Ampere-Reactive (MVAR)
Q_{Di}	Reactive power required at node i	Megavolt-Ampere-Reactive (MVAR)
e_i	Real part of the tiller tension i	Kilovolt (kV)
f_i	Imaginary part of the tension at the tiller i	Kilovolt (kV)
e_m	Real part of the tension at the tiller clearance m	Kilovolt (kV)
f_m	Imaginary part of the tension at the tiller clearance m	Kilovolt (kV)
Z_i	Internal impedance of the source	Ohm (Ω)
Z_l	Impedance of the line sections crossed	Ohm (Ω)
Z_a	Impedance of the equipment encountered	Ohm (Ω)
I_{cc}	Single-phase short-circuit current	Kilo-Ampere (kA)

List of acronyms and abbreviations

p.u: per unit
NIN: National Interconnected Network
JDB : Jeu De Barre
PV: Photovoltaic

1. Introduction

The use of hydrocarbons for energy production leads to the production of greenhouse gases that pollute the environment, in addition to their very rapid depletion, while the demand for energy continues to increase. Faced with all these challenges, BURKINA FASO has adopted energy transition policies by promoting and facilitating access to local renewable energy sources.

To address this, the construction of several solar photovoltaic power plants connected to the National Interconnected Network (NIN) in cities across the country is planned. Furthermore, SONABEL's network was designed according to a vertical organization in which energy transfers follow the so-called "top-down" pattern: production-transport-distribution, while the injection of energy from solar power plants requires a certain flexibility from the electrical networks due to the intermittency of the energy source of these plants. Given the amount of energy that these solar power plants will inject into the SONABEL network, it is clear that the levels of degradation of the network's voltage and frequency will be quite significant. In order to ensure the proper functioning of the electrical network after the construction of these solar photovoltaic power plants, it is imperative for SONABEL to adapt to this new production, which implies bi-directional operation and instability of its electrical system. The objective of our study is to perform simulations on the National Interconnected Network (NIN) with the "Digsilent Power Factory" software in order to identify the levels of voltage degradation and the additional short-circuit current contribution following this injection.

2. Materials and Methods

2.1. Mathematical Model

2.1.1. Power Flow Calculation Equation

The study of power flow is an essential step in the design and planning of power systems. These calculations are necessary for the planning of power exchange between generation centers and for dispatching. It is also essential for the evaluation of transient stability, dynamic stability and the estimation of the state of the network as well as for taking adequate measures for possible contingencies.

In an electrical network, the busbars are characterized by a set of four variables: the active and reactive powers P and Q, the voltage V and its phase shift angle ρ between current and voltage. Generally, two are known and the other two are to be determined. We are generally dealing with three types of nodes: load nodes, generator nodes and balance nodes or reference nodes. The Burkina Faso NIR is characterized by a mesh structure respecting the configuration (load nodes, generator nodes and reference nodes).
If we consider the network of the node in figure 1.

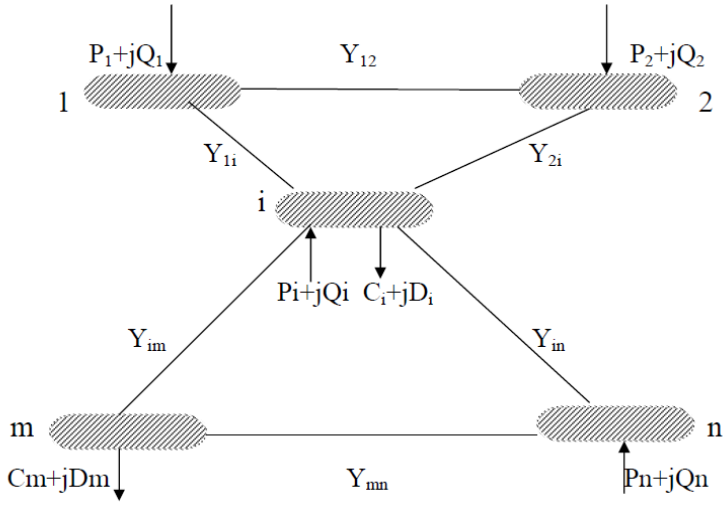

Figure 1: n-node network [1]

The apparent power at node "**i**" is given by the following relationship:

$$\boldsymbol{S_i = I_i^{*} V_i} \quad \textbf{(1)}$$

$$\textbf{Si = S}_{\textbf{Gi}}\textbf{- S}_{\textbf{Di}}\textbf{= (P}_{\textbf{Gi}}\textbf{- P}_{\textbf{Di}}\textbf{) + j (Q}_{\textbf{Gi}}\textbf{- Q}_{\textbf{Di}}\textbf{)} \quad \textbf{(2)}$$

The expression of the voltage at node **i** and **m** in its trigonometric form is:

$$\textbf{V}_{\textbf{i}}\textbf{= }|\boldsymbol{V_i}|\boldsymbol{e^{j\delta i}} \quad \textbf{(3)}$$

$$\textbf{Vm= }|\boldsymbol{V_m}|\boldsymbol{e^{j\delta m}} \quad \textbf{(4)}$$

Injecting expressions (3), (4), into equation (1), we get:

$$\boldsymbol{S_i} = \sum_{m=1}^{n}|\boldsymbol{V_i}|\, \boldsymbol{e^{j\delta i}(\rho_{im} - j\beta_{im})(|V_m|e^{-j\delta m})} \quad \textbf{(5)}$$

$$=|\boldsymbol{V_i}|\sum_{m=1}^{n}\boldsymbol{V_m}\left[\boldsymbol{\rho_{im}}[\cos(\boldsymbol{\delta i}-\boldsymbol{\delta m})+\boldsymbol{j}\sin(\boldsymbol{\delta i}-\boldsymbol{\delta m})]-\boldsymbol{j\beta_{im}}[\cos(\boldsymbol{\delta i}-\boldsymbol{\delta m})+\boldsymbol{j}\sin(\boldsymbol{\delta i}-\boldsymbol{\delta m})]\right] \quad \textbf{(6)}$$

By replacing S_i with expression (2) above, we obtain:

$$\begin{cases}\boldsymbol{P_{Gi}-P_{Di}=V_i\sum_{m=1}^{n}V_m\,[\rho_{im}\cos(\delta i-\delta m)+\beta_{im}\sin(\delta i-\delta m)]}\\ \boldsymbol{Q_{Gi}-\ Q_{Di}=V_i\sum_{m=1}^{n}V_m\,[\rho_{im}\sin(\delta i-\delta m)-\beta_{im}\cos(\delta i-\delta m)]}\end{cases} \quad \textbf{(7)}$$

This system can be written as follows:

$$\begin{cases}\boldsymbol{V_i\sum_{m=1}^{n}V_m\,[\rho_{im}\cos(\delta i-\delta m)+\beta_{im}\sin(\delta i-\delta m)]+P_{Di}-P_{Gi}=0}\\ \boldsymbol{V_i\sum_{m=1}^{n}V_m\,[\rho_{im}\sin(\delta i-\delta m)-\beta_{im}\cos(\delta i-\delta m)]+Q_{Di}-Q_{Gi}=0}\end{cases} \quad \textbf{(8)}$$

These equations are non-linear, so they cannot be solved by the analytical method. The solution is obtained by numerical methods. This equation can be solved through several methods namely, the iterative method of Gauss Seidel, the Gauss Seidel method with acceleration, and the iterative method of Newton-Raphson. The method used by the software is the Newton-Raphson method because it requires only a few iterations even for large networks and has significant computing power.

The power flow equations relate voltage and power instead of voltage and current.

The active power losses P_L and reactive power losses Q_L are defined as:

$$\begin{cases}\boldsymbol{P_L=\sum_{i\neq m}^{n}[(P_{Gi}+P_{Gm})-(P_{Di}+P_{Dm})]}\\ \boldsymbol{Q_L=\sum_{i\neq m}^{n}[(Q_{Gi}+Q_{Gm})-(Q_{Di}+Q_{Dm})]}\end{cases} \quad \textbf{(9)}$$

with $P_{Gm}\ et\ Q_{Gm}$= active and reactive powers generated by the node m,
$P_{Dm}\ et\ Q_{Dm}$ = active and reactive powers requested by the node m.

Solving the power flow equations: Newton-Raphson method

Principle of the Newton Raphson method [15]

The method consists in introducing a sequence (x_n) of successive approximations of the equation $f(x) = 0$.

- We start with an x_0 close to the solution.
- From x_0, we calculate a new term x_1 in the following way: we draw the tangent to C_f at x_0. This tangent intersects the x-axis at x_1 as shown in the figure below.
- We repeat this process by calculating x_2 by replacing x_0 with x_1, then x_3 by replacing x_1 with x_2 and so on ....

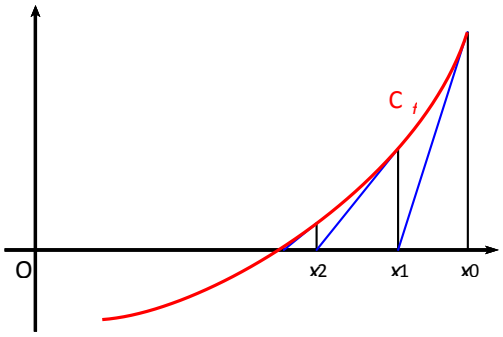

Conditions for the application of the Newton-Raphson method

For the sequence (x_n) to exist:

- The function f must be derivable at each of the points considered. In practice the function must be derivable in an interval centered in α containing x_0.
- The derivative must not cancel on this interval.

For the sequence (x_n) to be convergent, the conditions go beyond the senior class, but in practice, we must take an x_0 close enough to the value α that cancels the function. This is determined using the intermediate value theorem.

To allow the use of the NEWTON-RAPHSON method, we will reduce equation (10) to a form linking voltage and power,

Starting from equation (9),

And by posing: $$\begin{cases} \boldsymbol{e_i = V_i cos\delta_i} \\ \boldsymbol{f_i = V_i sin\delta_i} \\ \boldsymbol{e_m = V_m cos\delta_m} \\ \boldsymbol{f_m = V_m sin\delta_m} \end{cases} \quad \textbf{(10)}$$

We obtain: $$\begin{cases} \boldsymbol{P_i = \sum_{m=1}^{n}[e_i(e_m\rho_{im} + f_m\beta_{im}) + f_i(f_m\rho_{im} - e_m\beta_{im})]} \\ \boldsymbol{Q_i = \sum_{m=1}^{n}[f_i(e_m\rho_{im} + f_m\beta_{im}) + e_i(f_m\rho_{im} - e_m\beta_{im})]} \end{cases} \quad \textbf{(11)}$$

This system of equations is non-linear. The active power P_i and reactive power Q_i are known and the real and imaginary components of the voltage e_i and f_i are unknown for all busbars except the reference busbar where the voltage is specified and fixed. The NEWTON-RAPHSON method requires that the nonlinear equations be formed from expressions relating the powers and voltage components. [10]. This results in:

$$\begin{bmatrix} \Delta P_1 \\ \dots \\ \frac{\Delta P_{n-1}}{\Delta Q_1} \\ \dots \\ \Delta Q_{n-1} \end{bmatrix} = \left[\begin{array}{ccc|ccc} \frac{\partial P_1}{\partial e_1} & \dots & \frac{\partial P_1}{\partial e_{n-1}} & \frac{\partial P_1}{\partial f_1} & \dots & \frac{\partial P_1}{\partial f_{n-1}} \\ \dots & \dots & \dots & \dots & \dots & \dots \\ \frac{\partial P_{n-1}}{\partial e_1} & \dots & \frac{\partial P_{n-1}}{\partial e_{n-1}} & \frac{\partial P_{n-1}}{\partial f_1} & \dots & \frac{\partial P_{n-1}}{\partial f_{n-1}} \\ \hline \frac{\partial Q_1}{\partial e_1} & \dots & \frac{\partial Q_1}{\partial e_{n-1}} & \frac{\partial Q_1}{\partial f_1} & \dots & \frac{\partial Q_1}{\partial f_{n-1}} \\ \dots & \dots & \dots & \dots & \dots & \dots \\ \frac{\partial Q_{n-1}}{\partial e_1} & \dots & \frac{\partial Q_{n-1}}{\partial e_{n-1}} & \frac{\partial Q_{n-1}}{\partial f_1} & \dots & \frac{\partial Q_{n-1}}{\partial f_{n-1}} \end{array}\right] \begin{bmatrix} \Delta e_1 \\ \dots \\ \frac{\Delta e_{n-1}}{\Delta f_1} \\ \dots \\ \Delta f_{n-1} \end{bmatrix} \quad \textbf{(12)}$$

Equation (13) can be written as follows:

$$\begin{cases} P_i = e_i(e_i\rho_{ii} + f_i\beta_{ii}) + f_i(f_i\rho_{ii} + e_i\beta_{ii}) + \sum_{m=1,\ m\neq i}^{n} [e_i(e_m\rho_{im} + f_m\beta_{im}) + f_i(f_m\rho_{im} - e_m\beta_{im})] \\ Q_i = e_i(e_i\rho_{ii} + f_i\beta_{ii}) + f_i(f_i\rho_{ii} + e_i\beta_{ii}) + \sum_{m=1,\ m\neq i}^{n} [f_i(e_m\rho_{im} + f_m\beta_{im}) + e_i(f_m\rho_{im} - e_m\beta_{im})] \end{cases} \quad \textbf{(13)}$$

In this equation: *i is* the number of the bar set concerned and

m is the number of the production centre (generator)

This allows us to have:

$$\begin{cases} P_i^{(k+1)} = P_i^k + \Delta P_i \\ Q_i^{(k+1)} = P_i^k + \Delta Q_i \end{cases} \quad \textbf{(14)}$$

3.1.2. Short circuit current calculation equations

The sizing of an electrical installation and the materials to be used, the determination of the protection of people and goods, require the calculation of the short-circuit currents at any point of this network. The method of calculation of short-circuit currents applied in the software is the one proposed by the IEC 60909 standard. It deals with the case of radial and meshed circuits, LV - Low Voltage and HV - High Voltage. This standard is based on the théorème de Thévenin and consists in calculating an equivalent voltage source at the point of court-circuit. The calculation principle is a simple application of Ohm's law:

$$\textbf{Icc}=\frac{U}{Zi + \Sigma Zl + \Sigma Za} \quad \textbf{(15)}$$

3.2 Simulation assumptions

For these simulations, we will first calculate the penetration rates while considering the interconnections for each scenario. Then we will simultaneously inject the instantaneous powers of the different solar power plants at the chosen date of each year and observe the impact of these power fluctuations on the NIR in terms of power flow and short circuit currents. To do so, we will perform the following scenarios:

- **Scenario 1:** Initial state of the grid with only the Zagtouli solar plant and interconnections. In this reference case (current state of the grid), only the Zagtouli PV plant (33 MW) is in operation. In this case, the solar penetration rate calculated by equation 16 is 9.84%. The country's interconnections are 100 MW to Côte d'Ivoire and 100 MW to Ghana.

$$T_P = \frac{Pc}{Pp} \times 100\% \quad \textbf{(16)}$$

- **Scenario 2:** We solve the problems of the current grid in order to facilitate the injection of the production of these plants with the same initial conditions, while planning the integration of the future photovoltaic plants into the grid. The penetration rate is still 9.84%.
- **Scenario 3:** All plants are existing (in 2021) with their average production. We will calculate the penetration rate again using the same formula, using the 2021 peak estimated at 452.79 MW according to SONABEL data. This gives a penetration rate of 58.52%. In this scenario, we consider solar power plants at their average production time in order to see the impacts on voltage and short-circuit currents.
- **Scenario 4:** In this scenario, we still consider the network in the same state as scenario 3 but in this case, the power plants will be considered at their maximum power time.

3. Results and Discussion

3.1 Analysis of Power Flow Execution

The network has been modeled and all the equipment has been represented. The power flows (steady state) were calculated by the software based on the Newton-Raphson iteration law. The objective of these calculations is to determine:

- The voltages of the various nodes and their phase shifts with the current ;
- The active and reactive powers of the different branches ;
- The currents of the different branches ;

These power flows were run for all the different scenarios we have described in order to observe the changes in voltage, currents and power flows. In order to better understand these changes, we have chosen some nodes of the network (energy injection points of the solar PV plants) for the analyses.

Scenario 1: In this reference scenario (year 2018), the penetration rate is 10.98%. For this low renewable energy rate, the Zagtouli power plant alone cannot cause significant impacts on the grid. Several elements of the grid are in a state of overload:

- All of the network's generation centres are operating at more than 90% of their rated power and some are overloaded;
- Several busbars operate at voltages outside the permitted limits;
- Overloads on some transmission lines;
- Overloads in several transformers.

The electrical diagram of this simulation is attached in the following figure 2:

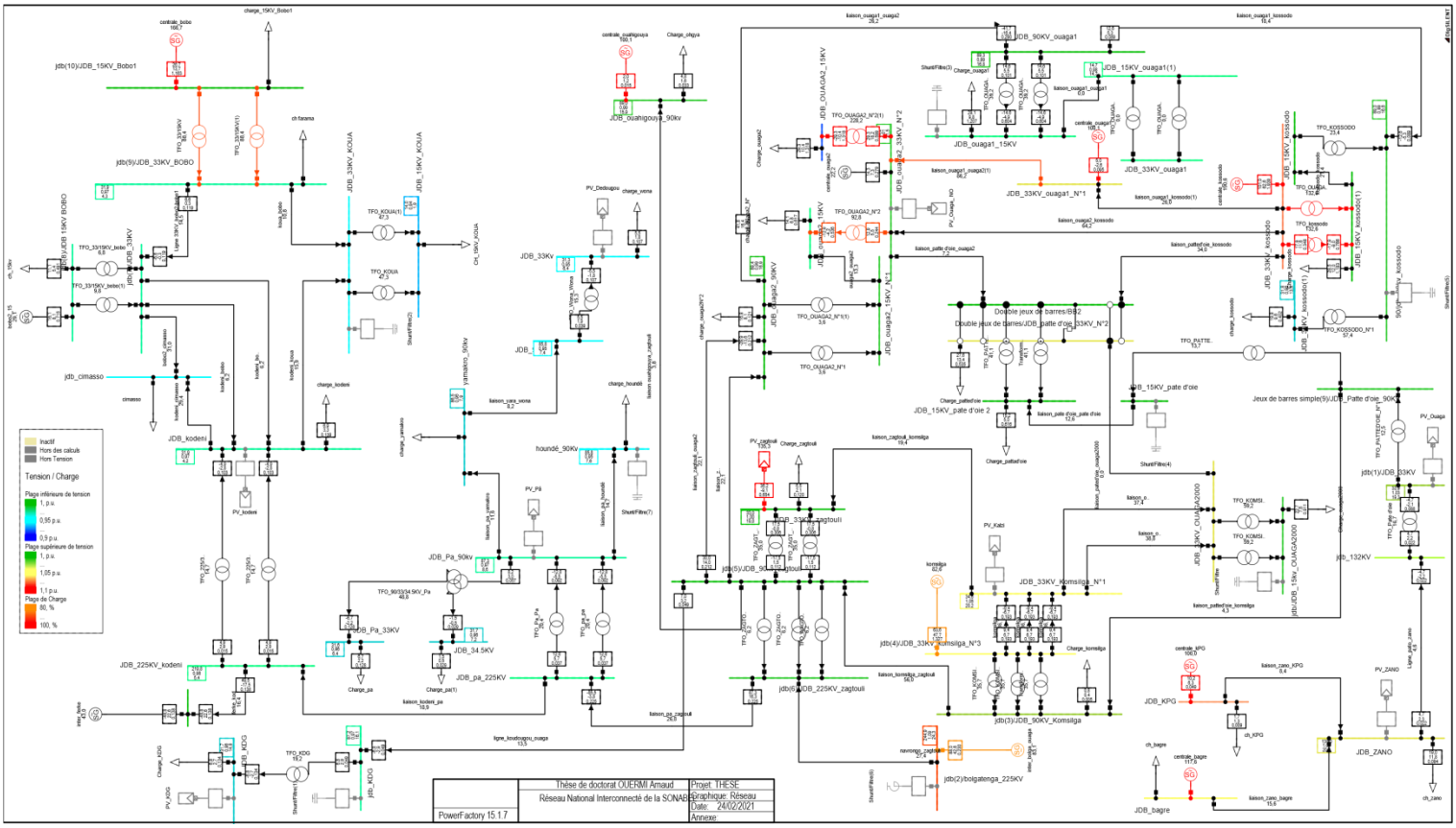

Figure 2: National Interconnected Network at initial state

In Figure 2, the complete circuit of the interconnected power system is shown (generating stations, power lines, busbars, transformers, circuit breaker, loads).

In the simulation result, the different elements of the network are coloured according to their load level as shown in the legend above. The red colour indicates that the element concerned is at least 100% overloaded.

Note that the same principles will be considered for the interpretation of future simulation results.

The list of network elements operating outside the permitted range is given in the following tables 1 and 2:

Table 1: Equipment (JDB busbars) operating outside the permitted ranges

Names	Voltages in p.u	Voltages in kV
Jdb_33 kV_kossodo	1.07	35.38
Jdb_15 kV_ouaga2	0.91	13.62
Jdb_132 kV_Kompienga	1.07	141.25
Jdb_225 kV_Bolgatenga	1.09	244.90

Table 2: Equipment (lines, transformers and generating stations) operating outside the permitted ranges

Names	Expenses as a % of total
Link_ Ouaga1_Ouaga2	86.2
TFO_Ouaga2_N ^{0}2_33/15 kV	92.83
TFO_Ouaga2_N^{0} 2 (1) _33/15 kV	228.21
2 TFO_KOSSODO_33/15 kV	132.63
2 TFO_Bobo1_33/15 kV	88.4
PV_zagtouli	135.33
Central_bobo2	166.67
Central_bagre	117.65
Central_kpga	100
Central_kossodo	190.58
Central_ouaga1	100
Central_Ouahigouya	100

The overloads observed on these different elements of the National Interconnected Network of Burkina Faso show that the network already presents problems in terms of power flow before the injection of the planned solar photovoltaic plants.

All overloaded grid elements require reinforcement for the proper functioning of the initial grid before the massive integration of intermittent energy sources.

We also note that in this scenario, if all the national generating stations, Agrecko and the interconnections provide their maximum power, a power of 48.8 MW is exported to Cote d'Ivoire.

Scenario 2: In this operation, the network reinforcements have been completed and the network is ready to receive future solar power plants. The completed reinforcements are as follows:

- Change to double ring for the Ouaga1_ Ouaga2 link lines
- Increase of the power of the two 33/15 kV transformers of Bobo1 from 10 MVA to 15 MVA each.
- Increase of the power of the two 33/15 kV transformers of KOSSODO from 15 MVA to 50 MVA each.
- Increase of the power of the two 33/15 kV transformers TFO Ouaga2 N ^{0}2 (1) and TFO Ouaga2 N ^{0}2 from 15 MVA to 50 MVA each
- Connection of a 10 MVAr capacitive shunt filter on the 33 kV busbar of Koua;
- Connection of a 10 MVAr shunt filter on the 90 kV busbar of Koudougou;
- Connection of a 20 MVAr capacitive shunt filter on the 90 kV busbar of Houndé;
- Connection of a 5 MVAr capacitive shunt filter on the 15 kV busbar of ouaga 2000;
- Connection of a 20 MVAr inductive shunt filter on the 225 kV busbar at the bolga interconnection.
- Shutdown of the Komsilga power plant to help reduce overloads on the busbars and reverse the flow of energy to Cote d'Ivoire, which is now imported at a rate of 16.8 MW.
- After integrating the various corrections, the simulation report shows that no busbar, line or transformer is overloaded on the power system; the persistent overloads at the generation plants can be solved by increasing their installed power.
- We can then start inserting the solar PV plants into this healthy network in order to simulate their impact on it.

Scenario 3: We are in the year 2021 while all the planned plants are installed and the penetration rate is 53.65%. At this penetration rate, the grid is highly dependent on the output of these solar plants, so their impacts start to be felt on the grid. In this scenario, we assume that all solar power plants operate simultaneously at their average power. The power of the different plants was calculated from equation 17, which we programmed in an Excel workbook using the sunshine and temperature data of typical years in the month of March, exactly at 11:00 am (maximum production time of the plants) of that year;

$$\boldsymbol{P = S \times N \times G \times \eta} \quad \textbf{(17)}$$

The 2021 peak load data at busbar level was used.

The capacity of the plants at that time is shown in the following Table 3:

Table 3: Average power output of solar PV plants (between 10:00 and 15:00)

Sites of the power plants	Zagtouli 50MWp	Koudougou	Dédougou	Ouaga NO	Zano	Kalzi	Pâ	Kodeni	Ouaga
Instantaneous power in MW	24.26	9.38	8.74	23.29	9.38	17.45	17.45	17.45	117.45

The following table 4 shows the different changes in power and voltage flows that occurred as a result of the average power injection of the solar photovoltaic plants.

Table 4: Comparison of power flow parameters for scenarios 2 and 3

Parameters	Voltages in p.u		Active power in MW		Reactive power in MVAr	
Control point	Scenario2	Scenario3	Scenario2	Scenario3	Scenario2	Scenario3
Jdb_kmsilga_33 kV	0.98	1.11	-10.8	-22.2	-3.6	-13.2
Jdb_Zano_132 kV	1.02	1.08	5.8	5.4	2.9	4.1
Jdb_33 kV_ KDG	0.99	1.12	-7.3	1.9	-2.9	2
Jdb_33 kV (wona)	0.98	1.09	-6.0	8.7	-1.9	6.4
Jdb_33 kV_Zagtouli	1.00	1.04	19.6	35.8	8	-14.6
Jdb_Ouaga2_33 kV	0.99	1.05	45.3	64.6	20.4	32.8
Jdb_Pa_90 kV	1.01	1.07	-19.8	-9.8	11.8	29.5
Jdb_kodéni_33 kV	1.01	1.04	-14.6	-16.2	2.8	2.2

The following curves illustrate the variations in voltage, active power and reactive power due to the injection of energy from solar power plants during their operation at average power.

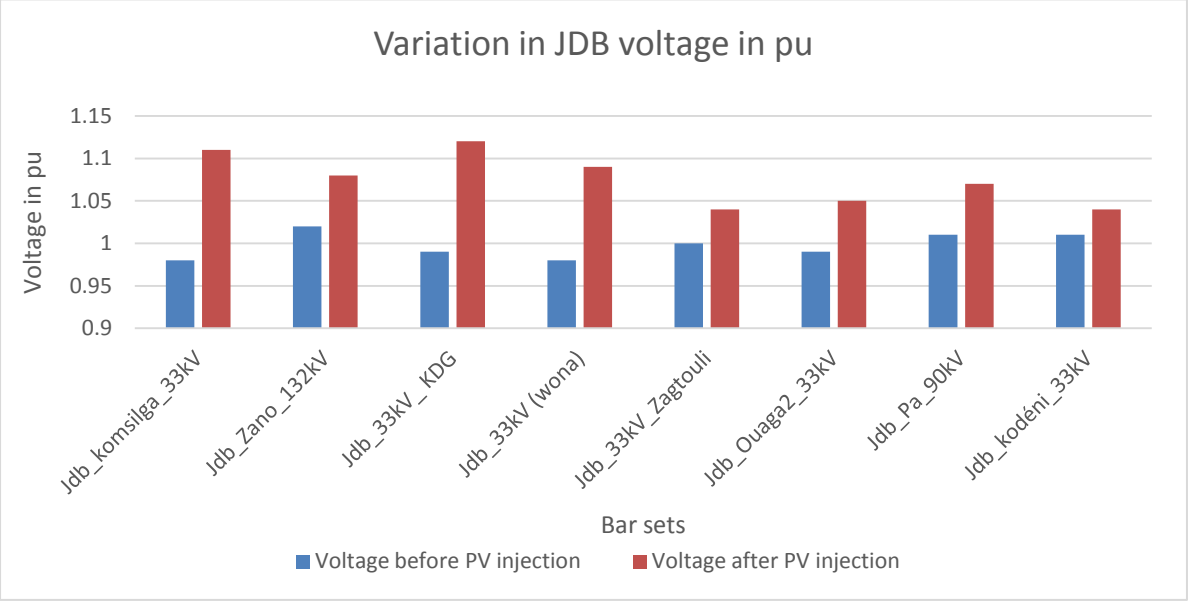

Figure 3: Voltage variation following the injection of the average power of the solar power plants

After the injection of energy from the solar photovoltaic plants, we note that the busbars of Komsilga, Zano, Koudougou, Wana, and Pâ are outside the voltage range accepted by SONABEL ([0.95pu-1.05pu]). These voltage variations do not allow for optimal operation of the electrical network.

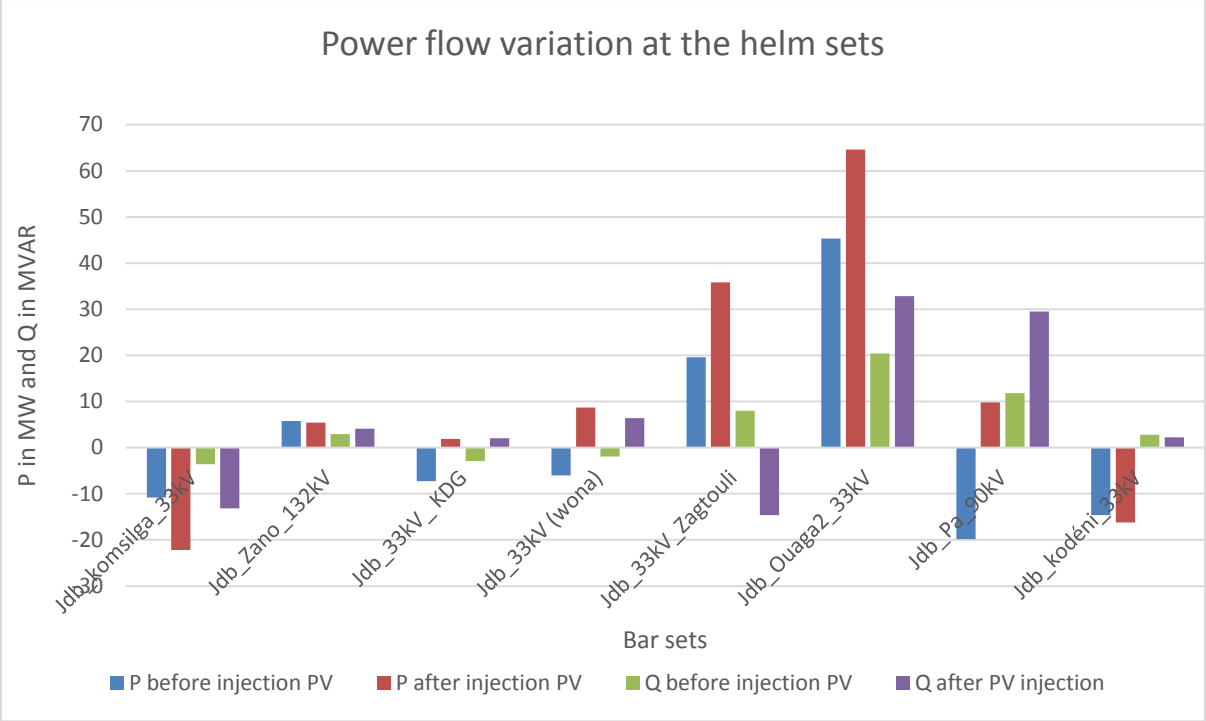

Figure 4: Variations in power flows following the injection of the average power of solar power plants

The analysis of the graph shows that following the injection of energy from the solar power plants, the power flows are greatly modified (increase, decrease and reversal of direction) at the level of the majority of the busbars. These modifications require the electrical network to readjust its protection equipment and to modernise the SONABEL dispatching centre and communication system.

Scenario 4: In this scenario, we are still in the same conditions as in scenario 3, but in this case, the power plants are at their maximum productions and their powers at the maximum operating times are quoted in the following table 5:

Table 5: Maximum production capacity of solar photovoltaic plants

Power Plant Sites	Zagtouli 50 MWp	Koudougou	Dédougou	Ouaga NO	Zano	Kalzi	Pâ	Kodeni	Ouaga
Instantaneous power in MW	36.89	14.77	11.08	29.53	14.77	22.13	22.13	22.13	22.13

The following table shows the level of change in voltage and power flows as a result of the maximum power injection of the solar power plants.

Table 6: Comparison of power flow parameters for scenarios 2 and 4

Parameters	Voltages in p.u		Active power in MW		Reactive power in MVAr	
Control point	Scenario2	Scenario4	Scenario2	Scenario4	Scenario2	Scenario4
Jdb_zagtouli_33 kV	1	1	19.6	37	8	-22.4
Jdb_kdgou_33 kV	0.99	1.10	-7.3	2.4	-2.9	2.2
Jdb_33 kV (wona)	0.98	1.10	-6.00	8.7	-1.9	8.3
Jdb_ouaga2_33 kV	0.99	1.03	45.3	63.8	20.4	32.5
Jdb_zano_132 kV	1.02	1.11	5.8	6.2	2.9	5
Jdb_kmsilga_33 kV	0.98	1.08	-10.8	-21.6	-3.6	-15
Jdb_pâ_90 kV	1.01	1.05	-19.8	10.4	11.8	26
Jdb_kodeni_33 kV	1.01	1.03	-14.6	-14.8	2.8	2.6

The results of this scenario show overloads at several transformers and an increase in grid instability following the injection of the maximum power of these solar plants on the grid. The following graphs show the levels of voltage degradation and power flow changes following this maximum injection.

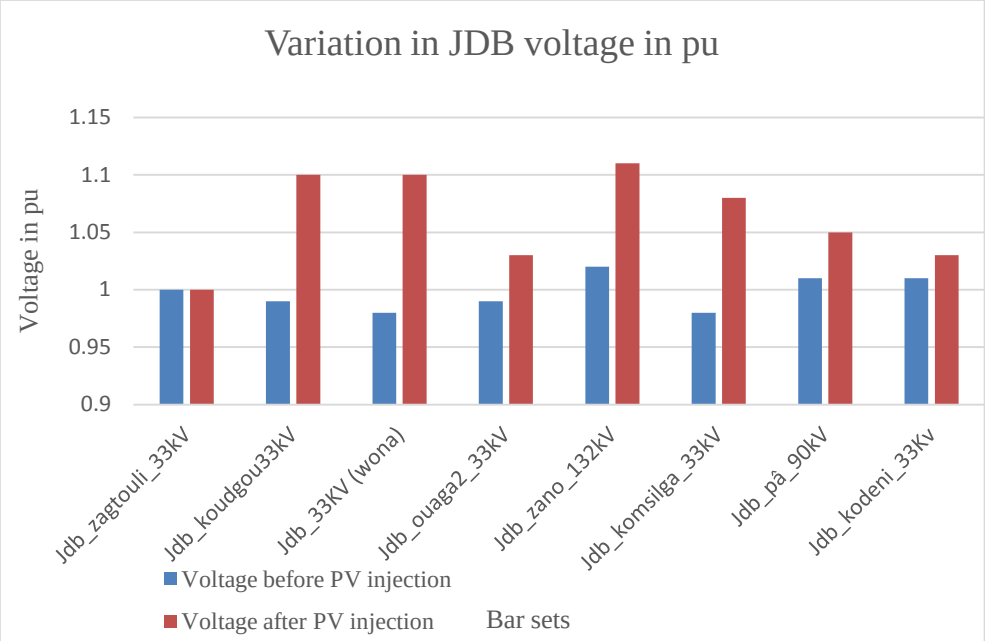

Figure 5: Voltage variations following the injection of the maximum power of solar power plants

The analysis of this graph shows an instability characterized by the degradation of the voltages (overvoltage) of most of the busbars. As the production of these power plants (solar PV) is variable and intermittent, permanent voltage variations will occur at the busbar level. As shown in the previous graph, these voltages may exceed the limits allowed by the network ($0.95\ Un \leq U \leq 1.05\ Un$ for the transmission networks and $0.93\ Un \leq U \leq 1.07\ Un$ for the distribution network) this situation may cause the protections to trip.

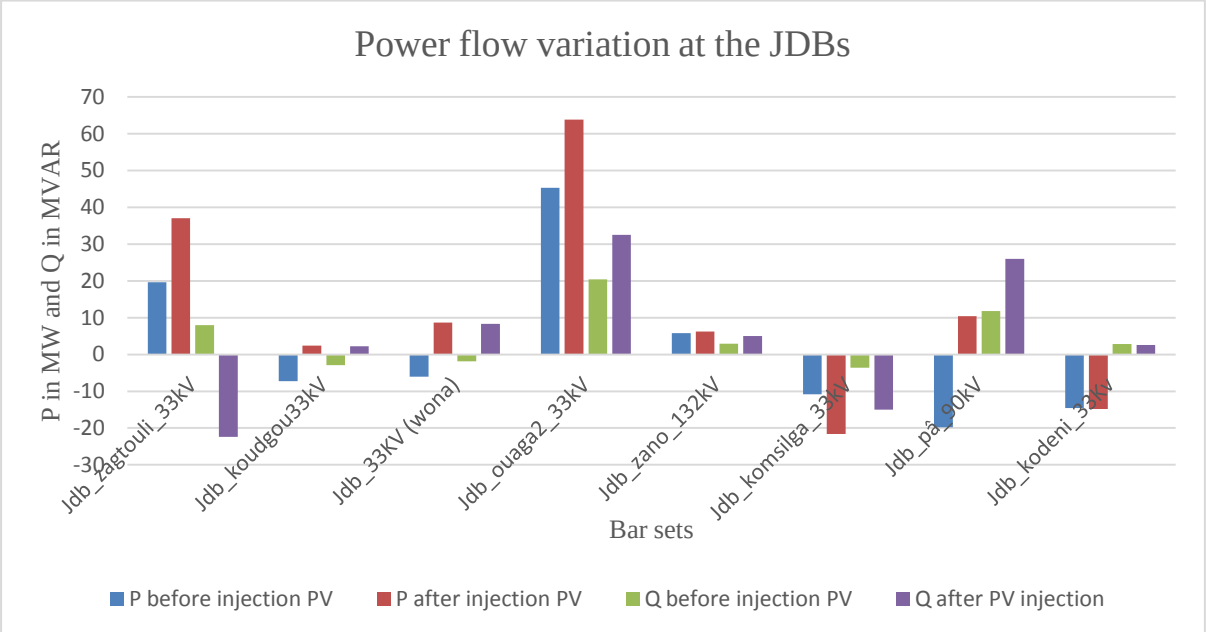

Figure 6: Variations in power flows following the injection of the maximum power of solar power plants

At this level of production, we also note that Côte d'Ivoire, which was an electricity supplier, now draws an active power of 55.2 MW and a reactive power of 1.6 MVAr from the SONABEL network through the Ferké bar set. This phenomenon shows the importance of interconnections.

The power flows are greatly modified (increase, decrease and inversion of direction) at the level of the majority of the busbars. These modifications require the electrical network to readapt its power and protection equipment, as well as to modernise the SONABEL dispatching centre and communication system.
The following actions were taken to achieve an acceptable level of stability (in terms of busbar tension):

- Shutdown of the Komsilga thermal power plant (65 MW),
- Shutdown of the Bagré hydroelectric plant (16 MW)
- The two 33/15 kV Kossodo transformers, the TFO Ouaga2 $N^0$2 (1) and TFO Ouaga2

N ^{0}2 15/33 kV transformers are increased from 50 MVA to 70 MVA each

- Disconnection of the 20 MVAR capacitive shunt filter at the 90 kV Houndé busbar
- Disconnection of the 10 MVAR capacitive shunt filter at the 90 kV busbar of Koudougou
- connection of a 15 MVAR capacitive shunt filter to the 15 kV busbar of Ouaga1
- connection of a 15 MVAR capacitive shunt filter to the 90 kV Kossodo busbar
- connection of a 5 MVAR inductive shunt filter to the Wona 33 kV busbar

Generation plants are overloaded and require reinforcement.

3.2 Analysis of the execution of the short-circuit currents of the different scenarios

This calculation was performed according to the IEC 60909 standard and its objective is to determine :

- The short-circuit powers in each branch and level of each node of the network;
- The peak short-circuit current (instantaneous value) ;
- The permanent short circuit current ;

The simulation of the short-circuit current calculation has been performed and it has allowed to highlight the impact of PV plants. To better enumerate these impacts, we have collected the short-circuit currents for the same points as those used for the power flow analysis in the following comparative table.

Table 7: Comparison of the short-circuit currents of scenarios 2, 3 and 4

Parameters / **Control point**	**Short circuit power Sk'' in MVA**			**Short circuit current Ik''. in KA**		
	Scenario2	**Scenario3**	**Scenario 4**	**Scenario2**	**Scenario3**	**Scenario 4**
Jdb_zagtouli_33 kV	544.39	697.2	742.7	10.58	12.2	13
Jdb_kdgou33 kV	119.22	124.2	124.5	2.09	2.13	2.18
Jdb_33kV (wona)	130.69	132	132.1	2.29	2.31	2.31
Jdb_ouaga2_33 kV	798.52	905.16	906.28	13.97	15.84	15.86
Jdb_zano_132 kV	228.36	262.63	233.19	1	1.15	1.02
Jdb_kmsilga_33 kV	466.65	987.61	1028.17	8.16	17.28	18
Jdb_pâ_33kV	162.02	542.6	544	2.83	3.49	3.49
Jdb_kodeni_33 kV	603.35	608.66	609	10.56	10.65	10.65
Jdb_Patte d'oie_33 kV	152.21	305.5	298.3	5.45	5.34	5.22
Jdb_ouaga1_90 kV	768.92	1030.2	1051.2	4.93	6.6	6.74

The above table shows the variations of the short-circuit currents during the variation of the power injected by the solar power plants in the electrical network. These variations affect the different protections of the electrical network because these will tend to be triggered during the progression of the power injected by the solar power plants. Moreover, if a short-circuit occurs during the period of maximum production of the solar power plants, the breaking capacity of the different protection equipments will not be able to support the short-circuit power; this phenomenon can cause the melting of the protection elements and possibly fires. Hence the need to resize the different protection elements of the electrical network.

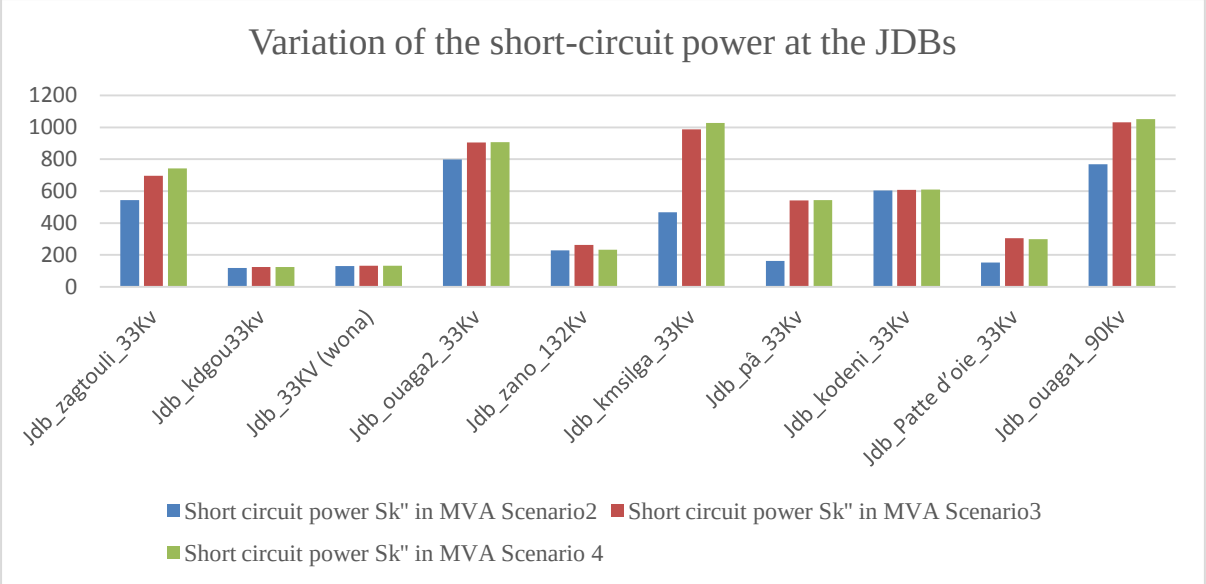

Figure 7: Variation of the short-circuit power following the injection of the energy produced by the solar power plants for the different scenarios

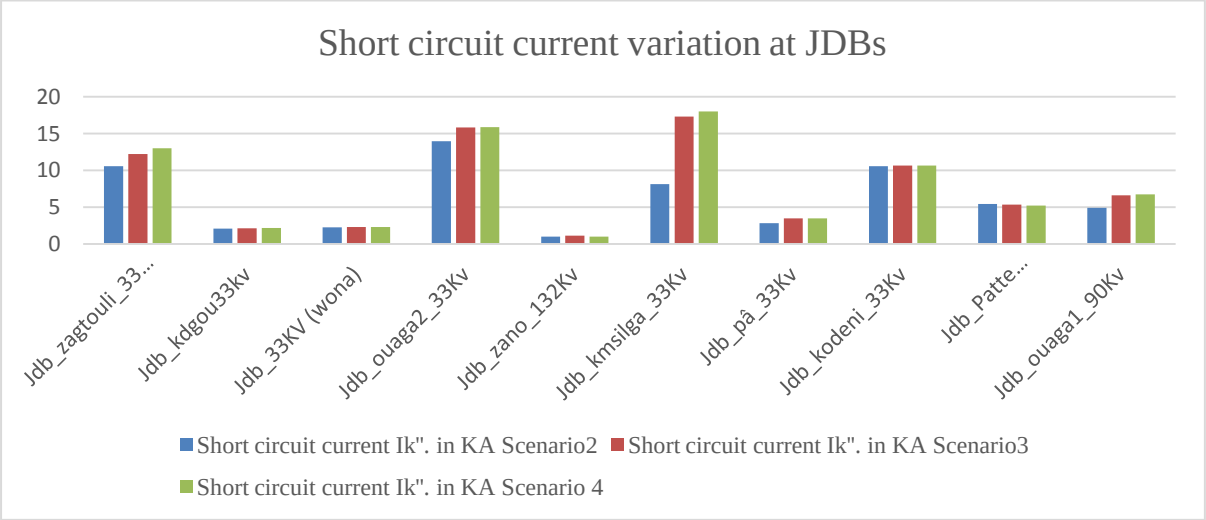

Figure 8: Variation of the short-circuit current following the injection of the energy produced by the solar power plants for the different scenarios

3.3 Proposed solutions to the problems observed during the simulations

The results of the different scenarios we have carried out show that SONABEL's current network will show instabilities following the massive insertion of renewable sources. Reinforcements are therefore necessary to ensure the stability and continuity of the network's operation; these reinforcements are among others

- Replace the two 33/15 kV Kossodo transformers of 50 MVA each with transformers with a minimum capacity of 70MVA-33 kV/15kV.
- Replace the TFO Ouaga2 N^0 2 (1) and TFO Ouaga2 N^0 2 15 MVA-15/33 kV transformers of OUAGA2 by transformers with a minimum power of 70 MVA-33 kV/15 kV ;
- Replace the two 10 MVA-33/15 kV transformers in Bobo1 with transformers with a minimum capacity of 15 MVA - 33 kV/15 kV;
- The Ouaga1-Ouaga2 link will be double terns;
- connection of a 15 MVAR capacitive shunt filter to the 15 kV busbar of Ouaga1
- connection of a 15 MVAR capacitive shunt filter to the 90 kV Kossodo busbar

- connection of a 5 MVAR inductive shunt filter to the Wona 33 kV busbar
- connection of a 10 MVAR capacitive shunt filter to the 33 kV busbar of KOUA
- connection of a 20 MVAR inductive shunt filter to the 225 kV Bolgatenga busbar
- connection of a 5 MVAR capacitive shunt filter to the 15 kV busbar of Ouaga 2000
- Increase in the power of the various overloaded generating stations according to their respective overload rates listed in Appendix 3.

The solutions we have proposed above make it possible to solve the problem of static stability and network overload. To solve the problem of dynamic stability of the network, SONABEL's network must be more flexible and move towards a smart grid.

4. Conclusion

The static stability study of the NIN after the injection of the solar power plants reveals instabilities in terms of power flow and short circuit currents such as overloading of some transformers, busbars or transmission lines, increases in short circuit currents. Reinforcements (increase in the section of overloaded lines, increase in the power of overloaded transformers or busbars, etc.) have been proposed in order to restore all the elements of the network in overloaded states to their normal operating ranges.

Dynamic studies (transient and on-load) are needed to inform us about the behaviour of the network in the face of an instantaneous disturbance.

References

[1]. Jimmy Royer, Thomas Djiako, et al, Le Pompage Photovoltaïque, Manuel de cours à l'intention des ingénieurs et des techniciens, IEPF/University of Ottawa/EIER/CREPA, 1998

[2]. Wendy Carolina Briceño Vicente, Raphaël Caire, Nouredine Hadjsaid. Possibilistic and probabilistic load distributions for uncertainty analysis. European Journal of Electrical Engineering, Lavoisier, 2015, 17 (3-4), pp.233 - 266. ⟨10.3166/ejee.17.233-266⟩. ⟨hal-01809965⟩

[3]. West African Power Pool Operating Manual : Decision N° 007/ERERA/15 adopting the West African Power Pool Operating Manual

[4]. Digsilent Power Factory Software Tutorial

[5]. E. Ouedraogo, O. Coulibaly, et al, Elaboration of a typical meteorological year of the city of Ouagadougou for the study of energy performance of buildings, University of Ouagadougou, March 2012

[6]. K. Kerkouche, F. Cherfa, A. Hadj Arab, et al, Evaluation of the global solar irradiation on a tilted surface according to different models for the Bouzaréah site, Centre de Développement des Energies Renouvelables, CDER, Alger, June 2013

[7]. Rezki Tadrist, Adnane Hassani, et al, Efficient FPGA Implementation to Estimate the Maximum output Power of Photovoltaic Panel Using Xilin System Generator, University of Blida, Algeria, May 2016

[8]. S. Conti, Analysis of distribution network protection issues in presence of dispersed generation, 'Electric Power Systems Rechearch, vol. 79, pp. 49-56, 2009.

[9]. N. Hadjsaid. Et al, La distribution d'énergie électrique en présence de production décentralisée - EGEM Génie Electrique, Lavoisier, Ed. Paris: Hermes Science, 2010.

[10]. O. LIyr Rowlands, Grid operation and stability report 2017-2035. Power Africa Transactions and Reforms Program (PATRP), USAID, May 2019

[11]. Ahmed Ousmane BAGRE, Brayima DAKYO, Yao Kétowoglo Azoumah, Coupling of photovoltaic power plants to unstable public grids: Application to the national grid of Burkina- Faso, , University of Le Havre, 2014

[12]. Tuan TRAN QUOC, Ch. Poraing, R. Feuillet, J.C. Sabonnadière, et al, Improvement of voltage stability on the vietman Power system, Laboratoire d'électrotechnique de Grenoble, 2000

[13]. International Standard IEC 60909-3, Short-circuit currents in three-phase alternating current systems, Second Edition 2003-09

[14]. Technical Report, IEC TR 60909-1, Short circuit current in three-phase a.c. systems, Second edition 2002-07
[15]. Paul MILAN, www.fourier.ujf-grenoble.